Supporting Information

Structural Dynamics of the Oxygen-Evolving Complex of Photosystem II in Water-Splitting Action

Andrew J. Wilson[1] *and Prashant K. Jain**[1,2,3]

[1]Department of Chemistry, University of Illinois at Urbana–Champaign, Urbana, Illinois 61801, United States

[2]Materials Research Lab, University of Illinois at Urbana–Champaign, Urbana, Illinois 61801, United States

[3]Department of Physics, University of Illinois at Urbana–Champaign, Urbana, Illinois 61801, United States

*Corresponding author Email: jain@illinois.edu

Table of Contents

Experimental Methods

Synthesis of Ag nanoparticles (NPs). Ag NPs were prepared according to the procedure by Lee and Meisel.[S1] First, 45 mg of $AgNO_3$ was dissolved in 250 mL of deionized water in an Erlenmeyer flask and brought to boiling conditions, under stirring. Separately, 50 mg of trisodium citrate was dissolved in 5 mL of deionized water in a 22 mL scintillation vial. After the $AgNO_3$ solution was boiled for 15 min, the 5 mL trisodium citrate solution was added drop-wise. The resultant solution was boiled and stirred for an additional 30 min. After ~15 min, the solution turned yellow-green indicating the formation of Ag NPs.

Photosystem II (PSII) isolation. Thylakoids were extracted from super-market spinach leaves, followed by isolation of PSII complexes using the Berthold-Babcock-Yocum (BBY) method.[S2]

Thylakoid extraction: Ninety-four grams of spinach were ground with 200 mL of 4-(2-hydroxyethyl)-1-piperazineethanesulfonic acid (HEPES) buffer (0.4 M NaCl, 20 mM HEPES, 4 mM $MgCl_2$, 5 mM ethylenediaminetetraacetic acid (EDTA), 1 mg/mL bovine serum albumin (BSA)) at pH 7.6. The suspension was then filtered with #4 filter paper. The filtrate was centrifuged at 6,000 *g* for 10 min. The pellet was resuspended in 120 mL of wash buffer (pH 7.6, 0.15 M NaCl, 20 mM HEPES, 4 mM $MgCl_2$, 1 mM EDTA, 1 mg/mL BSA) and centrifuged at 500 *g* for 1 min. The pellet was carefully removed and discarded. The remaining supernatant was centrifuged at 7,000 *g* for 10 min. The subsequent pellet was then resuspended in 80 mL of ethylene glycol (EG) buffer (pH 6.0, 15 mM NaCl, 20 mM 4-morpholineethanesulfonic acid (MES), 5 mM $MgCl_2$, 1 mM EDTA, 1 mg/mL BSA, 30 % (v/v) EG) and centrifuged for 10 min at 12,000 *g*, twice. The final pellet was suspended in 20 mL of EG buffer.

PSII complexes: Drop-wise, 0.8 mL of a suspension buffer (pH 6.0, 15 mM NaCl, 20 mM MES, 30% EG) was added to 4 mL of spinach thylakoids stirring in an ice bath. Next, 1.5 mL of Triton X-100 buffer (pH 6.0, 15 mM NaCl, 20 mM MES, 5 mM $MgCl_2$, 1 mM EDTA, 1 mg/mL BSA, 20 % (v/v) Triton X-100) was added drop-wise. The solution was continually stirred for 20 min in the dark. After stirring, the

thylakoid mixture was centrifuged at 37,000 *g* for 20 min. The pellet was resuspended in 8 mL of suspension buffer + 1 mL of Triton X-100 buffer, and centrifuged at 39,000 *g* for 20 min. The pellet was washed again with 9 mL of suspension buffer, centrifuged at 39,000 *g* for 20 min, and resuspended in storage buffer (pH 7.5, 0.4 M sucrose, 5 mM $MgCl_2$, 15 mM NaCl, 20 mM HEPES). The final solution containing PSII complexes was aliquoted into small volumes and stored in the freezer until use. PSII complexes were washed twice by centrifugation at 15,500 *g* for 7 min in deionized water prior to surface enhanced Raman scattering (SERS) measurements. For one of the control experiments, PSII prepared as above was then deliberately denatured. To accomplish denaturation, the solution containing PSII complexes was heated at 80 ºC for 1 h, prior to its drop-casting onto a SERS substrate.

Dissolved oxygen measurements of PSII. The oxygen-evolving activity of extracted PSII complexes was measured with a dissolved oxygen meter, results for which are summarized in Table S1. The PSII concentration was quantified in terms of the absorbance of chlorophyll (Chl).[S3] The PSII solution containing 0.4 M sucrose, 40 mM MES buffer (pH = 6.0), and 2 mM $[Fe(CN)_6]^{3-}$ as the electron acceptor[S4] was excited by 1.6 mW/cm^2 of 514.5 nm laser light for 1 h. The oxygen-evolving activity of this PSII solution was measured to be 1.8 ± 0.9 μmol O_2/mg Chl/h. When assayed in a solution containing 4 mM MES (pH = 6.0) and Ag NPs ($A_{415\ nm}$ = 1) as the electron acceptor, the PSII oxygen-evolving activity was found to be 5.7 ± 1.0 μmol O_2/mg Chl/h under excitation of 1.6 mW/cm^2 of 514.5 nm laser light. A lower solute concentration was required in the latter case to prevent precipitation of the Ag NPs. No oxygen evolution was measured in control studies, wherein a PSII solution (containing 0.4 M sucrose and 40 mM MES buffer (pH = 6.0), but no electron acceptor) or a Ag NP colloid solution (4 mM MES buffer, pH = 6.0, no PSII) was excited by 1.6 mW/cm^2 of 514.5 nm laser light for 1 h.

Sample preparation for SERS studies. Glass cover slips (VWR, No. 1 thickness) were cleaned by soaking in Piranha solution (3:1, H_2SO_4:30 % H_2O_2) for 1 h, profusely rinsing with water, and drying with N_2. Next, the cover slips were silanized with (3-aminopropyl)triethoxysilane by soaking in a 1.5 % ethanolic solution at 50 °C for 2 h. The slides were then rinsed with ethanol and water and dried with a stream of N_2. To form a SERS substrate, the functionalized slides were incubated in a solution of citrate-capped Ag NPs for a minimum of 12 h to allow electrostatic attachment between the amine and citrate moieties. After incubation, the slides were rinsed with water and dried with N_2. Since the Ag NPs were supported on a substrate, the citrate ligands, which enable colloidal dispersion, were no longer needed and were therefore removed by ultraviolet (UV) treatment. The Ag NP film was exposed to UV light from a Hg lamp for 7–15 min. This process results in the photo-oxidation of citrate to CO_2, leaving behind a relatively ligand-free or organic residue-free surface. Figure S4 shows representative SERS spectra from a Ag NP film before and after such UV treatment. The lack of SERS bands in the spectrum obtained post-UV treatment signify a relatively clean NP film surface that is free of ligands. Finally, PSII complexes were drop-cast and allowed to dry over the SERS substrate. The PSII complexes aggregate into discrete clusters (of varying size) on the SERS substrate, as seen in optical microscopy. An optical micrograph of one such cluster is shown in Figure S5 (inset). SERS spectra are obtained from a diffraction-limited region on one such PSII cluster.

Flow-cell construction for studies shown in Figure 1a. One millimeter diameter holes were drilled through opposite ends of a 1 mm thick glass slide (VWR). The glass slide was then cleaned by soaking in 2 M KOH at 150 °C for 1 h. Next, the slide was sonicated in deionized water for 30 min and dried with N_2. Two pieces of polyethylene tubing (150 mm length, 1.22 mm diameter) were inserted into the holes of the glass slide and sealed with epoxy on one side of the glass. After the epoxy dried, the excess tubing on the opposite side of the glass was cut flush with the glass surface. Finally, a glass coverslip substrate was coated with a film of Ag NPs and then treated with ultraviolet light from a Hg lamp for 7 min to photo-

oxidatively remove citrate ligands. This Ag NP film was overcoated with a sparse area density of clusters of PSII complexes. The sample-bearing cover slip was attached to the glass slide using epoxy and spacers to form a flow cell. The sample-bearing surface was enclosed within the flow cell. The flow cell was placed on an Olympus IX51 inverted microscope with the glass coverslip facing up. A 1 mW beam of a 514.5 nm Ar laser line was focused onto the sample using a 100X (UPlanoApo, 1.35 numerical aperture) microscope objective. The beam diameter (fwhm) was estimated to be 0.71 μm. Surface-enhanced Raman scattering (SERS) was collected with the same objective, filtered using a 514 nm RazorEdge® ultrasteep long-pass edge filter, and detected in the form of spectra using a Princeton Instruments Acton SP2300 spectrometer (1200 g/mm grating) coupled with a Princeton Instruments Pylon LN2-cooled CCD camera. The region of interest on the sample was aligned with the spectrometer slit. Integration time was set to 1 s. Signal from 10 vertical pixels around the region of interest was binned to increase S/N. SERS spectra were collected in a continuous manner before the start of water flow, during water flow, and after the end of water flow into the sample cell. It must be noted that the sample surface becomes defocused at the instant water enters the flow cell, due to pressure changes in the flow cell cavity. The sample surface eventually returns to focus after equilibration.

Raman scattering and SERS measurements. The substrate bearing the sample (PSII clusters only for Raman; Ag NPs + PSII clusters for SERS) was mounted on an Olympus IX51 inverted microscope. A 1-1.2 mW beam of a 514.5 nm Ar laser line was focused onto the sample using a 100X (UPlanoApo, 1.35 numerical aperture) microscope objective. The beam diameter (fwhm) was estimated to be 0.71 μm. SERS was collected with the same objective, filtered using a 514 nm RazorEdge® ultrasteep long-pass edge filter, and detected in the form of spectra using a Princeton Instruments Acton SP2300 spectrometer (1200 g/mm grating) coupled with a Princeton Instruments Pylon LN2-cooled CCD camera. PSII clusters, supported on either uncoated glass or on a Ag NP film substrate, were selected at random for Raman/SERS measurements. The region of interest on the sample was aligned with the spectrometer slit.

Spectra were collected in a continuous manner with acquisition time set to 1 s or 200 ms. Signal from 10 vertical pixels around the region of interest was binned to increase S/N. Solvent ($^{16}OH_2$ or $^{18}OH_2$) was introduced into the system by pipetting a few drops on top of the sample-bearing substrate.

Data processing and analysis

Sample selection and spectra plotting. PSII clusters, supported on either uncoated glass or on a Ag NP film substrate, were selected at random for Raman/SERS measurements. Raw spectra were acquired with WinSpec software, exported as ASCII files, and plotted using Origin software. Waterfall plots were plotted using MATLAB. Wherever normalized spectra are shown for improved presentation, the normalization was performed from 0 to 1.

Determination of Raman/SERS modes. A derivative analysis was conducted in MATLAB to determine the peak wavenumber of Raman/SERS modes from all spectra. First, each raw spectrum was smoothed using a Savitzky-Golay filter (span = 7, polynomial = 1). Next, an intensity derivative was calculated and smoothed using a Savitzky-Golay filter (span = 7, polynomial = 1). Zero-crossing points in the derivative plot were used to determine the peak wavenumber, provided the points match the following criteria: 1) the zero-crossing point lies on a negative sloping portion of the derivative curve and 2) the negative sloping portion of the derivative curve begins above a threshold set to 3X the standard deviation calculated between 1775–2168 cm^{-1}, where no modes are observed and only noise contributes. Histograms of tabulated Raman/SERS modes were constructed using a built-in MATLAB function with a bin size set to 3 cm^{-1}, which is 10X greater than the 0.3 cm^{-1} precision of detection.

Density functional theory (DFT) calculations

DFT calculations were performed using the software Gaussian 09. Oxygen-evolving complex (OEC) model geometries were built using the open-source Avogadro software. The charge for each intermediate

state was set on the basis of a net zero charge for S_0. High spin was set for all structures. Geometry optimizations and Raman mode calculations (mode frequencies, activity spectra, and free energies at 298.15 K and 1 atm) were performed with the B3LYP functional employing the LANL2DZ pseudo potential for Ca and Mn atoms and the 6-31G(d,p) basis set for O and H atoms. Interatomic distances were frozen during geometry optimizations (Figure S12). The polarizable continuum model was used to optimize the OEC geometries in water. Raman modes were calculated for $^{18}OH_2$ isotopologues by labeling only the oxygen atoms of the water ligands. OEC geometries, shown in figures, were plotted in the GaussView software.

Supporting Figures

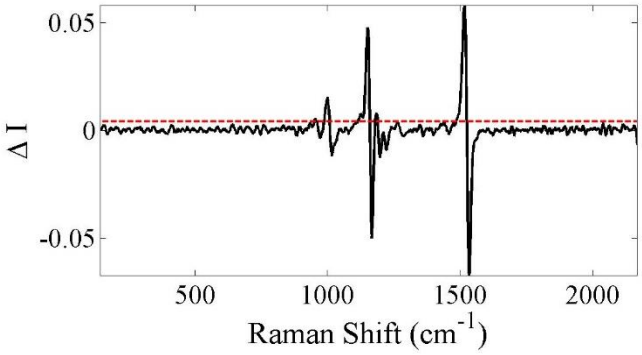

Figure S1. Spectral derivative and threshold. A representative plot of the intensity derivative of a Raman spectrum of glass-supported PSII clusters. The red dashed line indicates the threshold (3X standard deviation of the intensity between 1775–2168 cm^{-1}) set for determining zero-crossing points. Zero-crossing points are the spectral mode peak wavenumbers.

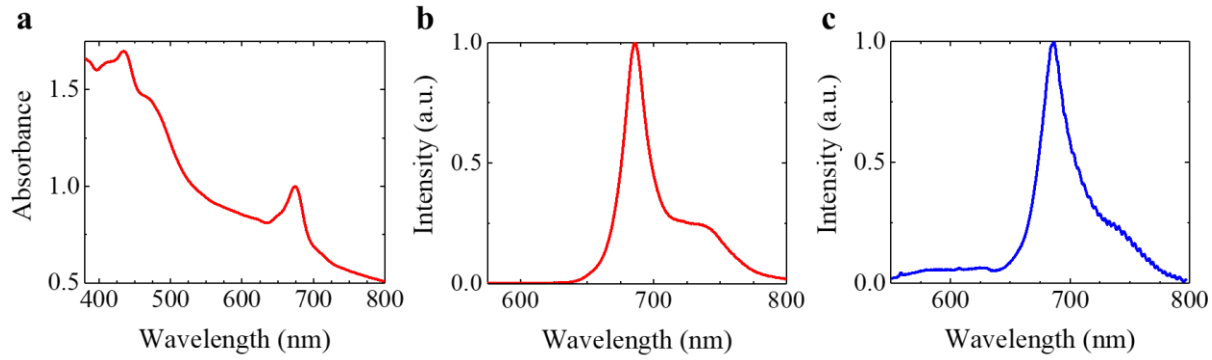

Figure S2. Bulk optical spectroscopy of PSII dispersions. (a) Representative absorbance spectrum of PSII dispersed in storage buffer (0.4 M sucrose, 5 mM $MgCl_2$, 15 mM NaCl, 20 mM 4-(2-hydroxyethyl)-1-piperazineethanesulfonic acid, pH 7.5). Chlorophyll absorption bands are observed with maxima at 434 nm and 674 nm. Accessory pigments absorb between 450 and 500 nm. (b) Representative normalized fluorescence spectrum of PSII complexes dispersed in ethylene glycol buffer (15 mM NaCl, 20 mM 4-morpholineethanesulfonic acid, 5 mM $MgCl_2$, 1 mM ethylenediaminetetraacetic acid, 1 mg/mL bovine serum albumin, 30% (v/v) ethylene glycol, pH 6.0) and excited with 0.8 mW of 514.5 nm light focused onto the dispersion with a 10X objective. The fluorescence band at 686 nm is a signature of chlorophyll *a*. Self-absorption of the fluorescence band at 686 nm is thought to excite vibrational sublevels of chlorophyll *a*, causing the red-shifted shoulder centered around 740 nm [ref S5]. (c) Representative normalized fluorescence emission spectrum from one PSII-containing region supported on a film of Ag NPs. A few drops of water were introduced atop the sample to provide an aqueous environment. The fluorescence band of PSII supported on the Ag NP film has a maximum at 686 nm, identical to the native PSII complexes in solution (b), which establishes the structural integrity[S6,S7] of PSII supported on the Ag NP film.

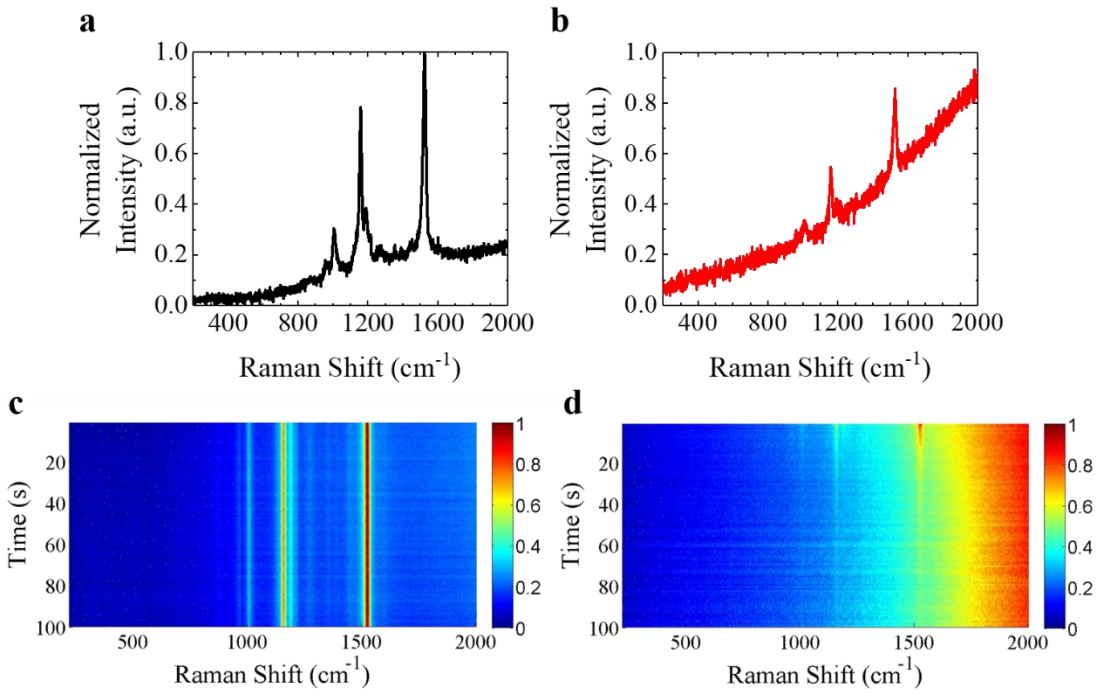

Figure S3. Raman spectroscopy of PSII on a glass substrate. Representative normalized Raman spectra of a glass-supported PSII cluster acquired in (a) air and (b) immersed in water. The Raman modes at 1524, 1157, and 1009 cm^{-1} are from β-carotene molecules[S8]. Waterfall plots (normalized from 0 to 1 across all spectra) of Raman spectra as a function of time, showing the stability of the Raman spectrum from PSII in (c) air and (d) immersed in water. The β-carotene Raman modes are stable in air, but they decrease in intensities in water due to the partial dissolution of β-carotene molecules within the excitation volume. Raman spectra were acquired from one PSII-containing region on the sample under focused 514.5 nm laser excitation power of 1 mW and a 1 s spectral acquisition. Dark counts were subtracted from the Raman spectra prior to normalization.

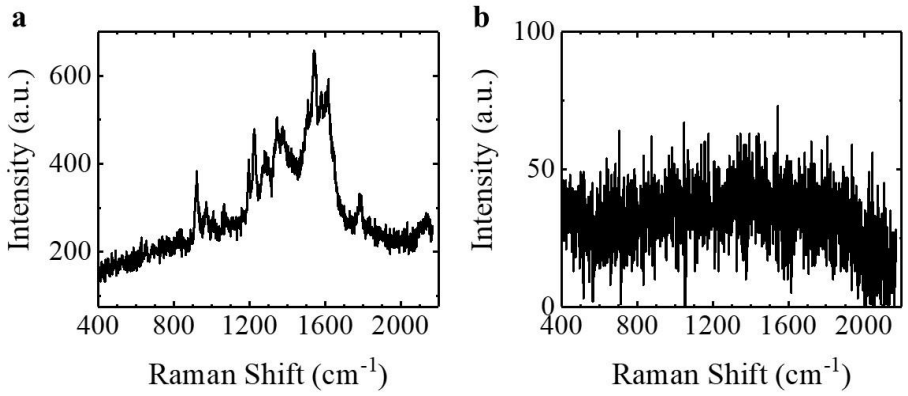

Figure S4. Background from SERS substrate. SERS spectrum of a film of Ag NPs on a glass coverslip substrate (a) before treatment and (b) following irradiation with ultraviolet (UV) lines from a Hg lamp for 7 min to photo-oxidatively remove citrate ligands from the NP surfaces. While SERS modes from citrate ligands appear in (a), the absence of these modes in (b) guarantees that in our studies of PSII on UV-treated Ag NPs, all SERS originates from PSII and not from the ligands on Ag NPs. SERS spectra were acquired from one Ag NP-containing region on the sample under focused 514.5 nm laser excitation of 1.1 mW power and a 1 s spectral acquisition.

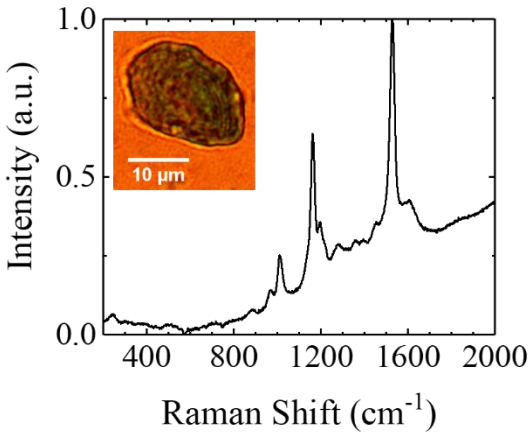

Figure S5. SERS spectrum of a PSII cluster in air. Sum of 100 SERS spectra collected from a diffraction-limited region of a cluster of PSII complexes on a Ag NP film. In this condition (absence of water), all organic SERS modes in PSII are located in the fingerprint region and no low-frequency modes (200–800 cm^{-1}) are observed. Inset is a representative optical micrograph of a cluster of PSII complexes. SERS spectra were acquired from a PSII-containing location on the SERS substrate under focused 514.5 nm laser excitation of 1 mW power and a 1 s spectral acquisition.

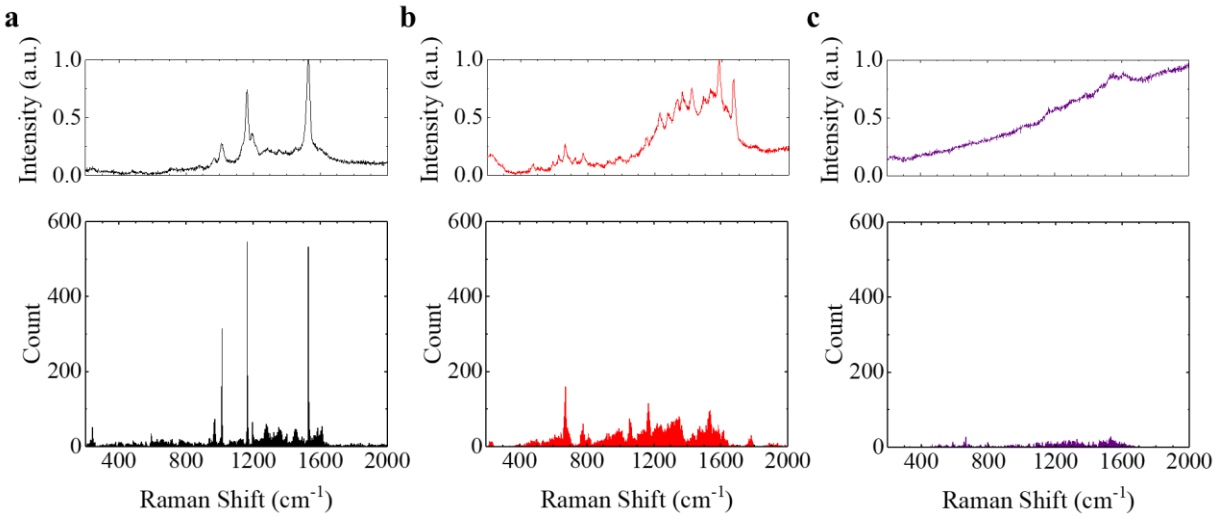

Figure S6. Histograms of PSII SERS modes in air and water. (a) A representative SERS spectrum (top) and mode distribution over 1000 such spectra (bottom) of PSII in air. β-carotene modes are most commonly observed, with no prominent modes in the low-frequency (200–800 cm^{-1}) region. (b) A representative SERS spectrum (top) and mode distribution over 1000 such spectra (bottom) of PSII in the presence of water. Unique modes, compared to those in air, are observed in both the fingerprint and low-frequency (200–800 cm^{-1}) regions. (c) A representative SERS spectrum (top) and mode distribution over 1100 such spectra (bottom) of denatured PSII in the presence of water. This control experiment shows that denatured PSII rarely exhibits any modes in either the low-frequency or fingerprint regions. SERS spectra were acquired from a PSII-containing location on the SERS substrate under focused 514.5 nm laser excitation of 1 mW power and a 1 s spectral acquisition. Histograms were generated using the procedure in the *Data processing and analysis* section.

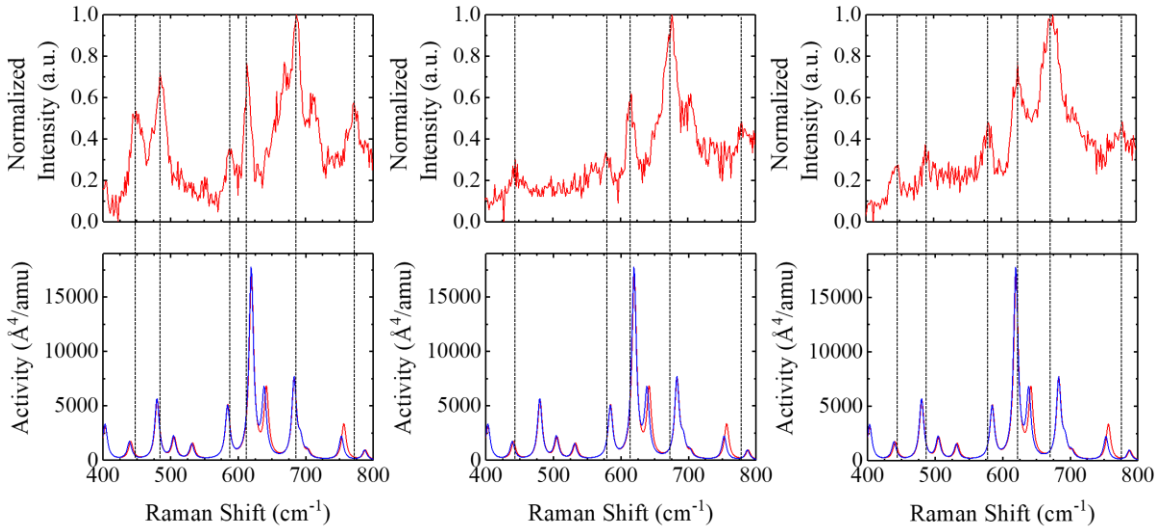

Figure S7. Examples of S_0. Examples of normalized SERS spectra of PSII assignable to the S_0 state (top, red). Each spectrum shown was selected from a continuous series of SERS spectra acquired with a 200 ms acquisition time in $^{16}OH_2$. Calculated Raman spectra (bottom panel, identical for all three columns) of the OEC in the S_0 state (W2 = H_2O and O5 = OH) with $^{16}OH_2$ (red) and $^{18}OH_2$ (blue) ligands. Vertical dashed lines are guides to demonstrate the match between modes of the experimental SERS spectra and those of the calculated Raman spectra. SERS spectra were acquired from a PSII-containing location on the SERS substrate under focused 514.5 nm laser excitation of 1.2 mW power.

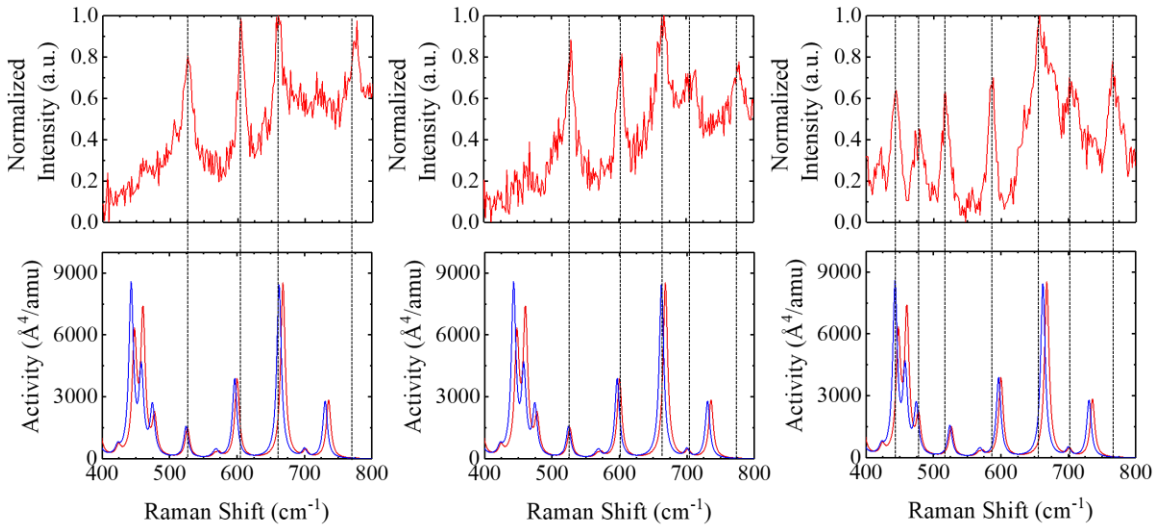

Figure S8. Examples of S_1. Examples of normalized SERS spectra of PSII assignable to the S_1 state (top, red). Each spectrum shown was selected from a continuous series of SERS spectra acquired with a 200 ms acquisition time in $^{16}OH_2$. Calculated Raman spectra (bottom panel, identical for all three columns) of the OEC in the S_1 state (W2 = H_2O and O5 = O) with $^{16}OH_2$ (red) and $^{18}OH_2$ (blue) ligands. Vertical dashed lines are guides to demonstrate the match between modes of the experimental SERS spectra and those of the calculated Raman spectra. SERS spectra were acquired from a PSII-containing location on the SERS substrate under focused 514.5 nm laser excitation of 1.2 mW power.

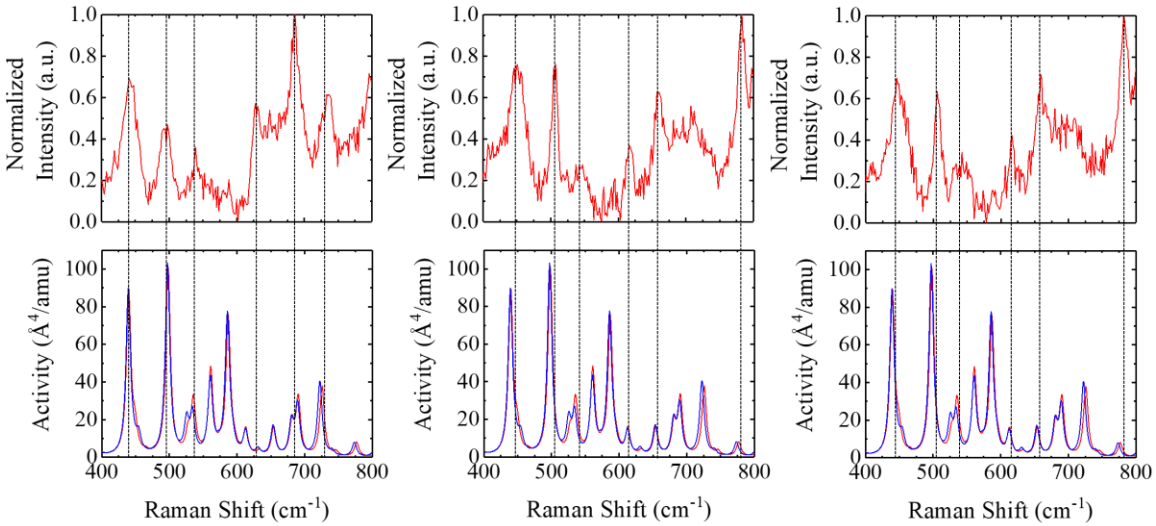

Figure S9. Examples of S_2 open cubane. Examples of normalized SERS spectra of PSII assignable to the S_2 open cubane state (top, red). Each spectrum shown was selected from a continuous series of SERS spectra acquired with a 200 ms acquisition time in $^{16}OH_2$. Calculated Raman spectra (bottom panel, identical for all three columns) of the OEC in the S_2 open cubane state with $^{16}OH_2$ (red) and $^{18}OH_2$ (blue) ligands. Vertical dashed lines are guides to demonstrate the match between modes of the experimental SERS spectra and those of the calculated Raman spectra. SERS spectra were acquired from a PSII-containing location on the SERS substrate under focused 514.5 nm laser excitation of 1.2 mW power.

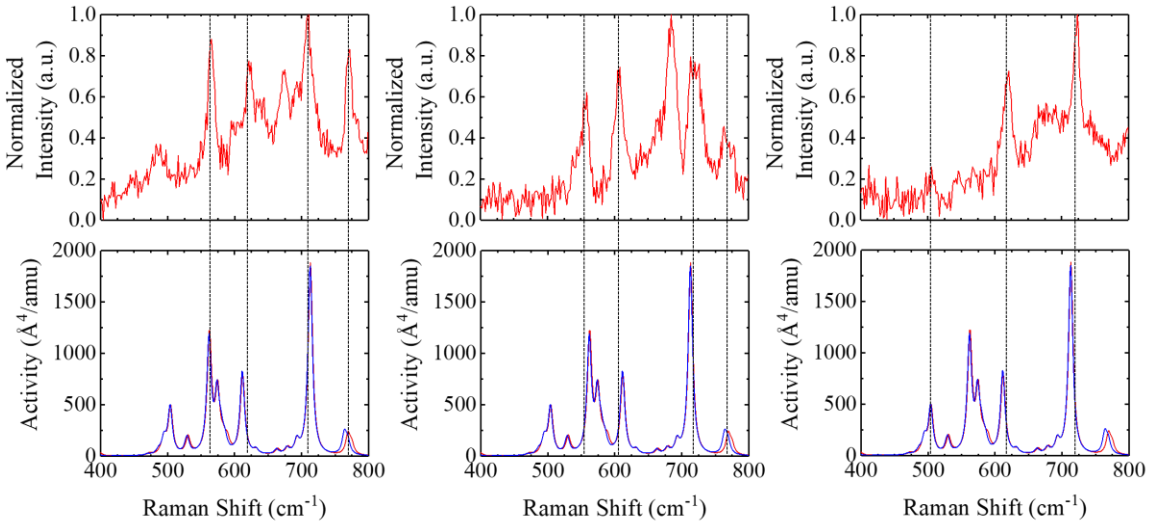

Figure S10. Examples of S_2 closed cubane. Examples of normalized SERS spectra of PSII assignable to the S_2 closed cubane state (top, red). Each spectrum shown was selected from a continuous series of SERS spectra acquired with a 200 ms acquisition time in $^{16}OH_2$. Calculated Raman spectra (bottom panel, identical for all three columns) of the OEC in the S_2 closed cubane state with $^{16}OH_2$ (red) and $^{18}OH_2$ (blue) ligands. Vertical dashed lines are guides to demonstrate the match between modes of the experimental SERS spectra and those of the calculated Raman spectra. SERS spectra were acquired from a PSII-containing location on the SERS substrate under focused 514.5 nm laser excitation of 1.2 mW power.

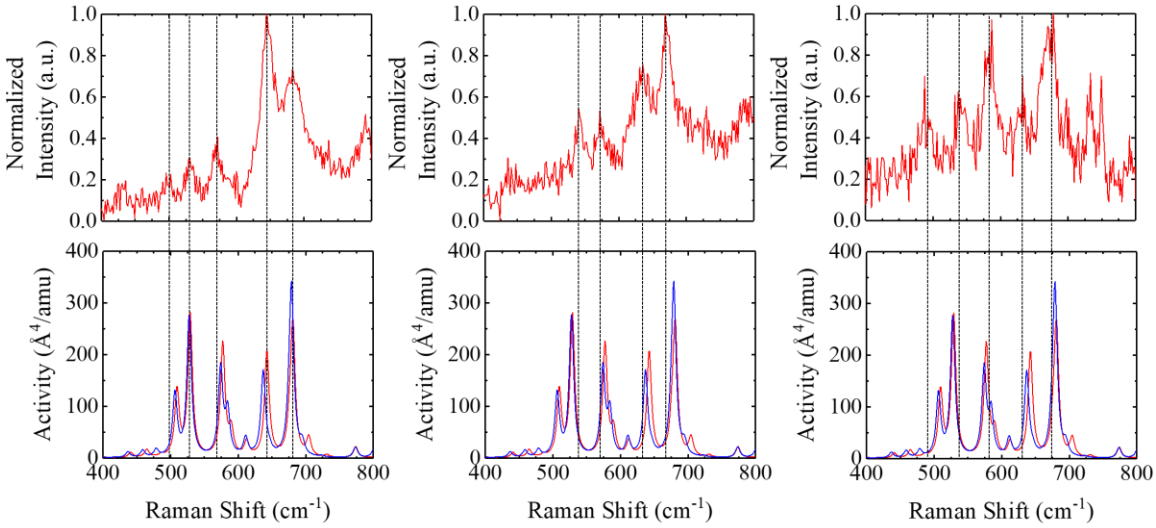

Figure S11. Examples of S_3 RH W_x. Examples of normalized SERS spectra of PSII assignable to the S_3 RH W_x state (top, red). Each spectrum shown was selected from a continuous series of SERS spectra acquired with a 200 ms acquisition time in $^{16}OH_2$. Calculated Raman spectra (bottom panel, identical for all three columns) of the OEC in the S_3 RH W_x state with $^{16}OH_2$ (red) and $^{18}OH_2$ (blue) ligands. Vertical dashed lines are guides to demonstrate the match between modes of the experimental SERS spectra and those of the calculated Raman spectra. SERS spectra were acquired from a PSII-containing location on the SERS substrate under focused 514.5 nm laser excitation of 1.2 mW power.

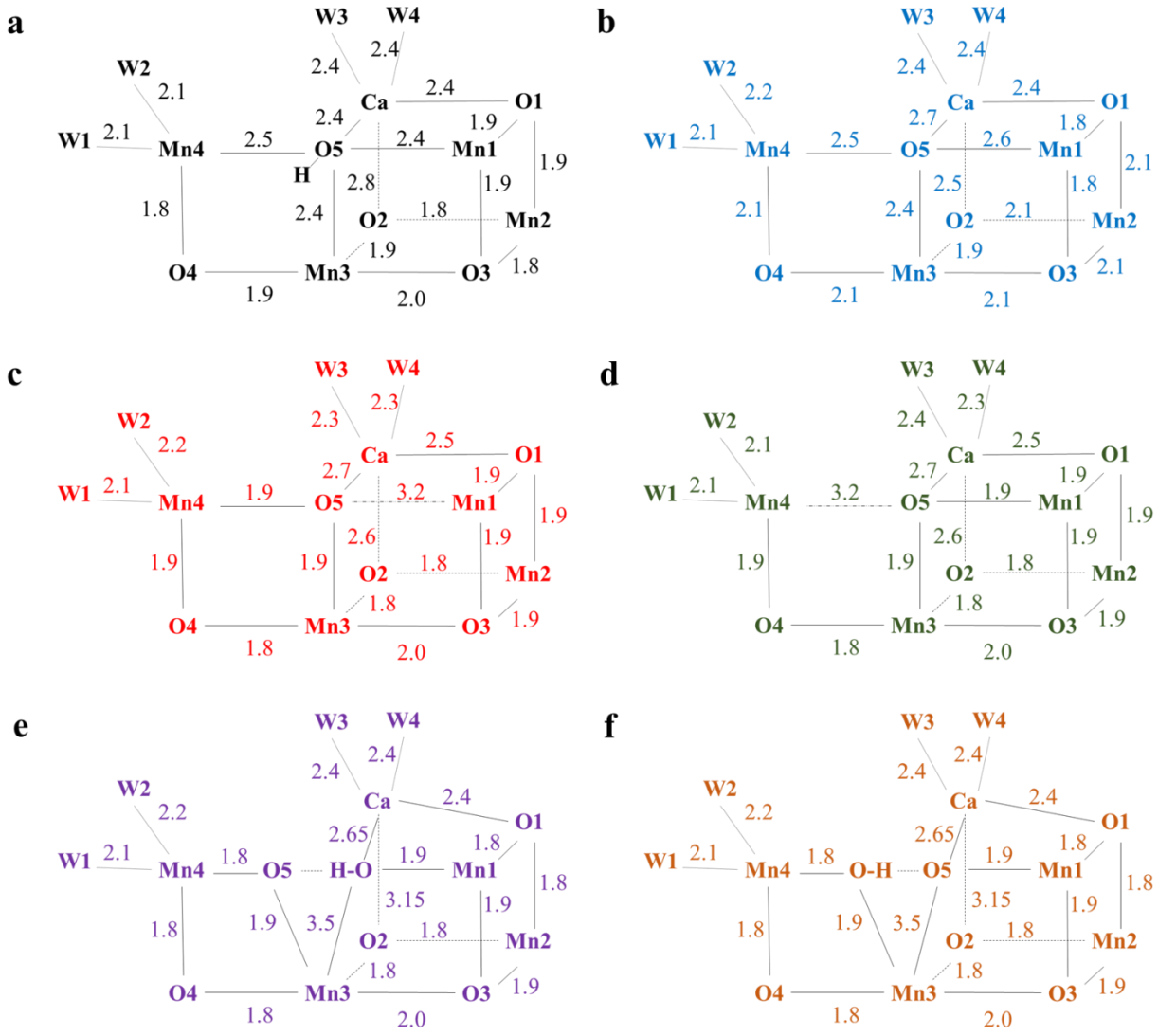

Figure S12. Interatomic distances (indicated in Å) of the OEC used in DFT calculations. (a) S_0 [ref S9], (b) S_1 [ref S10], (c) S_2 open cubane [ref S11], (d) S_2 closed cubane [ref S11], (e) S_3 RH W_x [ref S12], and (f) S_3 LH W_x [ref S12]. The elemental symbols have their usual meaning.

Table S1. Oxygen-evolving activity of PSII in solution (μmol O_2 · mg Chl^{-1} · h^{-1}) with an electron scavenger, under 514.5 nm laser excitation.

Electron acceptor	**$[Fe(CN)_6]^{3-}$**	**Ag NPs**	**none**
Trial 1	1.1	4.3	0
Trial 2	3.0	6.7	0
Trial 3	1.3	6.0	
Average	1.8	5.7	0
Standard Deviation	0.9	1.0	0

Table S2. Free energies (in eV) from DFT calculations.

S_2 open cubane	**-30862.9**
S_2 closed cubane	-30862.6
S_3 RH W_x	**-32926.2**
S_3 LH W_x	-32923.9

Supporting References

(S1) Lee, P. C.; Meisel, D. *J. Phys. Chem.* **1982**, *86*, 3391–3395.
(S2) Berthold, D. A.; Babcock, G. T.; Yocum, C. F. *FEBS Lett.* **1981**, *134*, 231–234.
(S3) Das, S. K.; Frank, H. A. *Biochemistry* **2002**, *41*, 13087–13095.
(S4) Büchel, C.; Barber, J.; Ananyev, G.; Eshaghi, S.; Watt, R.; Dismukes, C. *Proc. Natl. Acad. Sci.* **1999**, *96*, 14288.
(S5) Franck, F.; Juneau, P.; Popovic, R. *Biochim. Biophys. Acta, Bioenerg.* **2002**, *1556*, 239–246.
(S6) Chumanov, G.; Picorel, R.; Toon, S.; Seibert, M.; Cotton, T. M. *Photochem. Photobiol.* **1993**, *58*, 757–760.
(S7) Picorel, R.; Chumanov, G.; Cotton, T. M.; Montoya, G.; Toon, S.; Seibert, M. *J. Phys. Chem.* **1994**, *98*, 6017–6022.
(S8) Tracewell, C. A.; Cua, A.; Bocian, D. F.; Brudvig, G. W. *Photosynth. Res.* **2005**, *83*, 45–52.
(S9) Pal, R.; Negre, C. F. A.; Vogt, L.; Pokhrel, R.; Ertem, M. Z.; Brudvig, G. W.; Batista, V. S. *Biochemistry* **2013**, *52*, 7703–7706.
(S10) Umena, Y.; Kawakami, K.; Shen, J.-R.; Kamiya, N. *Nature* **2011**, *473*, 55–60.
(S11) Pantazis, D. A.; Ames, W.; Cox, N.; Lubitz, W.; Neese, F. *Angew. Chem. Int. Ed.* **2012**, *51*, 9935–9940.
(S12) Askerka, M.; Wang, J.; Vinyard, D. J.; Brudvig, G. W.; Batista, V. S. *Biochemistry* **2016**, *55*, 981–984.